AIMS Mathematics, 10(9): 21254–21272.
DOI:10.3934/math.2025949
Received: 11 December 2024
Revised: 07 August 2025
Accepted: 02 September 2025
Published: 16 September 2025

https://www.aimspress.com/journal/Math

Research article

Positivity and global existence for nonlocal advection-diffusion models of interacting populations

Valeria Giunta[1,*], Thomas Hillen[2], Mark A. Lewis[3] and Jonathan R. Potts[4]

[1] School of Mathematics and Computer Science, University of Swansea, Computational Foundry, Crymlyn Burrows, Skewen, Swansea SA1 8DD, UK

[2] Department of Mathematical and Statistical Sciences, University of Alberta, Edmonton, AB T6G 2G1, Canada

[3] Department of Mathematics and Statistics and Department of Biology, University of Victoria, PO Box 1700 Station CSC, Victoria, BC, Canada

[4] School of Mathematical and Physical Sciences, University of Sheffield, Hicks Building, Hounsfield Road, Sheffield S3 7RH, UK

* **Correspondence:** Email: valeria.giunta@swansea.ac.uk.

Abstract: We study a broad class of nonlocal advection-diffusion models describing the behaviour of an arbitrary number of interacting species, each moving in response to the nonlocal presence of others. Our model allows for different nonlocal interaction kernels for each species and arbitrarily many spatial dimensions. We prove the global existence of both non-negative weak solutions in any spatial dimension and positive classical solutions in one spatial dimension. These results generalise and unify various existing results regarding existence of nonlocal advection-diffusion equations. We demonstrate that solutions can blow up in finite time when the detection radius becomes zero, i.e. when the system is local, thus showing that nonlocality is essential for the global existence of solutions. We verify our results with numerical simulations on 2D spatial domains.

Keywords: nonlocal advection; positivity of PDEs; global existence; blow-up; numerical PDEs
Mathematics Subject Classification: 35A01, 35B09, 35B65, 35R09

1. Introduction

We consider a multispecies model of interacting species, which sense their environment and other species in a nonlocal way [15, 32, 37]. The individual populations are denoted by $u_i(x,t)$, where $t \geq 0$ denotes time, $x \in \Omega$ denotes space and the index $i = 1, \ldots, N$ denotes the species. The model is given

by

$$\partial_t u_i = D_i \Delta u_i + \nabla \cdot \left(u_i \sum_{j=1}^{N} \gamma_{ij} \nabla (K_{ij} * u_j) \right), \qquad i = 1, \ldots, N. \tag{1.1}$$

Here, K_{ij} is a twice-differentiable function, with $\nabla K_{ij} \in L^\infty$, and $K_{ij} * u_j$ denotes a convolution operator defined as

$$K_{ij} * u_j(x) = \int_\Omega K_{ij}(x - y) u_j(y) dy.$$

From a biological perspective, K_{ij} describes the nonlocal sensing of species j by species i. The constants $D_i > 0$ are diffusion coefficients of species i and the values of γ_{ij} denote the extent to which species i avoids (if $\gamma_{ij} > 0$) or is attracted to (if $\gamma_{ij} < 0$) species j. For the definition of the nonlocal term to make sense, here we let $\Omega = \mathbb{T}^n$, the n-torus defined by identifying the boundaries of $[-L_1, L_1] \times \cdots \times [-L_n, L_n]$ in a periodic fashion.

Nonlocal interaction models, such as (1.1), have become important tools in the mathematical modelling of biological species [3, 4, 11, 29, 32, 40]. Key to their specification are the nonlocal kernels, K_{ij}, which model the interactions within and between species. Organisms do not typically make movement decisions only based on the local information they have about prey, predator, or food sources. Rather, movement decisions are based on information gathered over a certain 'perceptual radius' via sight, smell, sounds, or other means of sensing [37]. These biological considerations have given rise to certain popular functional forms for the kernels, such as the top hat kernel, whereby K_{ij} is constant on a ball of radius R_{ij} around the origin and zero elsewhere, so that R_{ij} directly corresponds to an organism's perceptual radius [35]. Other works have considered exponentially decaying or normally-distributed kernels [14]. From the mathematical perspective, different choices of K_{ij} have sometimes been made for mathematical convenience, to enable either exact calculations [7] or proofs [28]. However, often there are only small modifications required to move between a biologically-inspired kernel (e.g. the top hat distribution) and a mathematically convenient one (e.g. a smooth mollification of the top hat kernel, allowing for certain existence proofs [17]). Here, we assume that each K_{ij} is integrable and twice differentiable with $\max_{i,j} \|\nabla K_{ij}\|_\infty < \infty$, which encompasses all the examples just mentioned, possibly up to an arbitrarily small mollification. Importantly, however, our assumption does not encompass the Dirac delta function, where nonlocality vanishes.

Currently, the mathematical analysis of organism movement based on nonlocal perception is at full swing [32]. Several authors consider models of the form (1.1) to study species aggregation, segregation, avoidance, home ranges, territories, mixing, and spatio-temporal patterns [3, 5, 6, 8, 12, 16, 18, 20, 27, 32, 34, 37]. In many of these papers, the analysis starts with results on local and global existence and positivity. These results are generated through various methods, such as energy functionals [6, 18, 28, 32], semigroup theory and fixed-point arguments [4], or direct PDE-type estimates [24], all depending on the specific model at hand. In [6], using methods from [9], the authors consider model (1.1) for one species with smooth interaction kernel and they show global existence of classical solutions, using energy-entropy methods. In [28] the assumption of smooth interaction kernels is relaxed, and assuming a detailed balance condition on the kernels, global existence for weak solutions is shown. Our previous work in [17] proves existence of local solutions in any space dimension and global solutions in 1D for the case of equal interaction kernels, i.e. $K_{ij} = K$.

Here we combine these results into a unifying existence theory for nonlocal models of type (1.1). In contrast to previous models, we allow the interaction kernels K_{ij} to vary from species to species, and

we have no restriction on the space dimension. This is somewhat surprising, since global existence for local versions of our model do strongly depend on the spatial dimension [10, 30, 38]. This behaviour is similar to the well known chemotaxis model [22, 26]. Solutions to the standard chemotaxis model are globally bounded in 1-D, while they blow-up in higher dimensions, if the initial population is large enough in the $L^{n/2}$-norm, where n denotes the space dimension [26]. Guided by these observations, we consider the local limit of (1.1) and we also find cases in $n \geq 2$ dimensions where finite time blow-up is possible.

The paper is organised as follows. In Section 2 we define a modified version of Equation (1.1) and prove some preliminary results. This modified model is then analysed in Section 3, where we prove the local existence of mild solutions, and in Section 4, where we prove the global existence of positive solutions. We conclude our proof by showing that every positive solution of the modified model is also a solution of Equation (1.1). In Section 5 we show that in the corresponding local system the solutions can blow up in finite time. Section 6 concludes with numerical simulations showing that the solutions of the nonlocal problem, although they become steeper as the detection radius becomes smaller, still remain bounded.

2. A modified version of our system

To establish our existence results for Equation (1.1), our approach is first to prove existence and non-negativity of weak solutions to a slightly modified version of Equation (1.1). We then show that any solution of this modified system is also a solution of Equation (1.1). The modified system is as follows

$$u_{it} = D_i \Delta u_i + \nabla \cdot \left(h(u_i) \sum_{j=1}^{N} \gamma_{ij} \nabla (K_{ij} * u_j) \right), \qquad i = 1, \ldots, N, \tag{2.1}$$

where $h(u) = u$ if $u \geq 0$ and $h(u) = 0$ if $u < 0$. Note that whenever $u_i \geq 0$, Equations (1.1) and (2.1) are identical. In Equation (2.1), derivatives are understood weakly. In particular, the weak derivative of $h(u)$ is $h'(u) = 1$ if $u > 0$ and $h'(u) = 0$ if $u < 0$. We collect some basic properties of $h(u)$ in the following Lemma.

Lemma 1. *For any $v \in H^1(\mathbb{T})$, we have $\|h(v)\|_{L^2} \leq \|v\|_{L^2}$, $\|\nabla h(v)\|_{L^2} \leq \|\nabla v\|_{L^2}$, and $\|h(v)\nabla v\|_{L^1} \leq \|v \nabla v\|_{L^1}$. For any $v_1, v_2 \in L^2(\mathbb{T})$, we have $\|h(v_1) - h(v_2)\|_{L^2} \leq \|v_1 - v_2\|_{L^2}$.*

Proof. The inequality $\|h(v)\|_{L^2} \leq \|v\|_{L^2}$ follows from the definitions of h and the L^2-norm. The inequality $\|\nabla h(v)\|_{L^2} \leq \|\nabla v\|_{L^2}$ follows from the same definitions, and also that $\nabla h(v) = h'(v)\nabla v$. The inequality $\|h(v)\nabla v\|_{L^1} \leq \|v \nabla v\|_{L^1}$ follows from the definitions of h and the L^1-norm.

For the final inequality, we observe that

$$\|h(v_1) - h(v_2)\|_{L^2}^2 = \int_{\mathbb{T}} (h(v_1(x)) - h(v_2(x)))^2 \mathrm{d}x = \int_{S_1} (v_1(x) - v_2(x))^2 \mathrm{d}x + \int_{S_2} v_1^2(x) \mathrm{d}x + \int_{S_3} v_2^2(x) \mathrm{d}x,$$

where $S_1 = \{x \in \mathbb{T} : v_1(x) > 0, v_2(x) > 0\}$, $S_2 = \{x \in \mathbb{T} : v_1(x) > 0, v_2(x) \leq 0\}$, and $S_3 = \{x \in \mathbb{T} : v_1(x) \leq 0, v_2(x) > 0\}$. Now, for $x \in S_2$, we have $v_2(x) \leq 0$ and $v_1(x) > 0$ so $v_1(x) \leq v_1(x) - v_2(x)$, and then $v_1^2(x) \leq (v_1(x) - v_2(x))^2$. Similarly, for $x \in S_3$, we have $v_2(x) \leq v_2(x) - v_1(x)$ and $v_2^2(x) \leq (v_2(x) - v_1(x))^2$.

Hence

$$\int_{S_1}(v_1(x)-v_2(x))^2\mathrm{d}x+\int_{S_2}v_1^2(x)\mathrm{d}x+\int_{S_3}v_2^2(x)\mathrm{d}x\leq\int_{S_1\cup S_2\cup S_3}(v_1(x)-v_2(x))^2\mathrm{d}x\leq\|v_1-v_2\|_{L^2}^2,$$

so that $\|h(v_1)-h(v_2)\|_{L^2}\leq\|v_1-v_2\|_{L^2}$. □

3. Local existence of mild solutions

We begin by proving local existence of mild solutions to Equation (2.1).

Definition 1. *Given* $u_0=(u_{10},...,u_{N0})\in(L^2(\mathbb{T}^n))^N$ *and* $T>0$, *we say that* $u(x,t)=(u_1(x,t),...,u_N(x,t))\in L^\infty((0,T),L^2(\mathbb{T}^n))^N$ *is a* **mild solution** *of Equation* (2.1) *if*

$$u_i=e^{D_i\Delta t}u_{i,0}-\int_0^t e^{D_i\Delta(t-s)}\nabla\cdot\left[h(u_i)\nabla\left(\sum_{j=1}^N\gamma_{ij}K_{ij}*u_j\right)\right]ds \tag{3.1}$$

for each $0<t\leq T$, *where* $e^{D_i\Delta t}$ *denotes the solution semigroup of the heat equation* $u_{it}=D_i\Delta u_i$ *on* $\mathbb{T}^n$, *and* $u_{i,0}(x)=u_i(x,0)$ *is the initial condition.*

Theorem 2. *Assume* $u_0\in H^2(\mathbb{T}^n)^N$ *and each* K_{ij} *is twice differentiable with* $\max_{i,j}\|\nabla K_{ij}\|_\infty<\infty$. *For each* $u_0\in L^2(\mathbb{T}^n)^N$ *there exists a time* $T_*>0$ *and a unique mild solution of Equation* (2.1) *with* $u\in L^\infty((0,T_*),L^2(\mathbb{T}^n))^N$. *Moreover,* $u\in C^1((0,T_*),L^2(\mathbb{T}^n))^N\cap C^0([0,T_*),H^2(\mathbb{T}^n))^N$.

Proof. In [17, Theorem 3.6] we showed local existence of mild solutions for Equation (1.1) using a fixed point argument. In that case the sensing mechanism for each species was equal $K_{ij}=K$ for all $i,j=1,\ldots,N$ where K is twice differentiable. To prove the same result for variable K_{ij} is straightforward. It requires replacing each $\|\nabla K\|_\infty$ with $\max_{i,j=1,...,N}\|\nabla K_{ij}\|_\infty$. To prove this for Equation (2.1) rather than Equation (1.1) requires additionally employing the estimates on h from Lemma 1. Other than this, the proof remains unchanged from that in [17, Theorem 3.6] so we do not repeat it here. □

4. Global existence and positivity

Following the strategy of [17], we define a time T_* as follows. If $\|u\|_{L^1}$ is bounded for all time then let $T_*=\infty$. Otherwise $\|u\|_{L^1}\to\infty$ as $t\to T_{\max}$ for some time $T_{\max}\in(0,\infty)$. In this case, let T_* be the earliest time such that $\|u\|_{L^1}=2\|u_0\|_{L^1}$. Our aim is to establish existence and positivity up to time T_*, then use this to prove that $T_*<\infty$ leads to a contradiction. This means that $T_*=\infty$, establishing global existence of weak solutions. To show that $T_*=\infty$, we need the following positivity result.

Lemma 3. *Keep all assumptions from Theorem 2 and also assume* $u_i(x,0)\geq 0$ *in* $\mathbb{T}^n$ *for all* $i=1,\ldots,N$. *Then* $u(x,t)\geq 0$ *for solutions of Equation* (2.1) *for* $t\in(0,T_*)$. *Here we understand* $u\geq 0$ *a.e. in* $\mathbb{T}^n$ *component-wise.*

Proof. Suppose $u=(u_1,...,u_N)$ is a solution to Equation (2.1) and let us fix an index $i\in\{1,\ldots,N\}$. We use a standard idea of cutting off the negative part of the solution. Such a method has, for example, been used in [21] for chemotaxis models. We define the negative part as $u_i^-(x,t):=u_i(x,t)$ if $u_i(x,t)<0$

and $u_i^-(x,t) := 0$ if $u_i(x,t) \geq 0$, and we split the domain $\mathbb{T}^n$ as $J_-(t) = \{x \in \mathbb{T}^n : u_i(x,t) < 0\}, J_0(t) = \{x \in \mathbb{T}^n : u_i(x,t) = 0\}$, and $J_+(t) = \{x \in \mathbb{T}^n : u_i(x,t) > 0\}$. Since the L^2-norm of u_i is differentiable in time, we can write

$$\frac{d}{dt}\frac{1}{2}\|u_i^-(.,t)\|_{L^2}^2 = \int_{J_-(t)} u_i^- u_{it}^- dx + \underbrace{\int_{J_0(t)} u_i^- u_{it}^- dx}_{=0} + \underbrace{\int_{J_+(t)} u_i^- u_{it}^- dx}_{=0} = \int_{J_-(t)} u_i^- u_{it}^- dx. \tag{4.1}$$

Since $J_-(t)$ is an open set and u_i and its weak spatial derivatives are continuous and differentiable in time, we have $u_{it}^- = u_{it}$ and $\nabla u_i^- = \nabla u_i$, on $J_-(t)$. Then from Equation (2.1) we obtain

$$\begin{aligned}
\frac{d}{dt}\frac{1}{2}\|u_i^-(.,t)\|_{L^2}^2 &= \int_{J_-(t)} u_i^- \left(D_i \Delta u_i + \nabla \cdot \left(h(u_i) \sum_{j=1}^N \gamma_{ij} \nabla (K_{ij} * u_j) \right) \right) dx \\
&= -D_i \int_{J_-(t)} |\nabla u_i^-|^2 dx + \int_{\partial J_-(t)} u_i^- D_i (\nabla u_i \cdot \mathbf{n}) dS - \int_{J_-(t)} (\nabla u_i^-) \cdot \left[h(u_i) \sum_{j=1}^N \gamma_{ij} \nabla (K_{ij} * u_j) \right] dx \\
&+ \int_{\partial J_-(t)} u_i^- h(u_i) \sum_{j=1}^N \gamma_{ij} (\nabla (K_{ij} * u_j) \cdot \mathbf{n}) dS,
\end{aligned} \tag{4.2}$$

where dS is used to denote the boundary measure on $\partial J_-(t)$ and $\mathbf{n}$ denotes the outward normal vector on $\partial J_-(t)$. On $\partial J_-(t)$, we have $u_i^- = 0$, hence both boundary integral terms vanish. The third term on the right hand side also vanishes, since on $J_-(t)$ we have $h(u_i) = 0$. Hence we find

$$\frac{d}{dt}\frac{1}{2}\|u_i^-(.,t)\|_{L^2}^2 = -2D_i \left(\frac{1}{2}\|\nabla u_i^-(.,t)\|_{L^2}^2 \right) \leq 0.$$

Therefore $\|u_i^-\|_{L^2}^2$ is a Lyapunov function and when $\|u_i^-(.,0)\|_{L^2} = 0$ then $\|u_i^-(.,t)\|_{L^2}^2 = 0$ for all $t > 0$. □

Theorem 4. *Let $u_0 = (u_{10}, ..., u_{N0}) \in H^2(\mathbb{T}^n)^N$ and make the same assumptions as in Lemma 3. Then in the solution from Theorem 2, we have $T_* = \infty$. In other words, $u \in C^1((0,\infty), L^2(\mathbb{T}^n))^N \cap C^0([0,\infty), H^2(\mathbb{T}^n))^N$.*

Proof. Since $u_i(x,t) \geq 0$ for all x, t, we have, for each $t \geq 0$,

$$\|u_i\|_{L^1} = \int_{\mathbb{T}} u_i(x,t) dx. \tag{4.3}$$

However, the right-hand integral (total population size) remains constant over time. Therefore $\|u_i\|_{L^1}$ is constant over time. Now recall the definition of T_*, which states that if $\|u_i\|_{L^1}$ is bounded for all i then $T_* = \infty$. □

This establishes global existence of weak positive solutions to Equation (2.1). To establish the analogous result for Equation (1.1), we note that any positive solution to Equation (2.1) is also a positive solution to Equation (1.1), since $h(u_i(x,t)) = u_i(x,t)$ whenever $u_i(x,t) \geq 0$. Hence we have established the following.

Theorem 5. *The solution $u \in C^1((0,\infty), L^2(\mathbb{T}^n))^N \cap C^0([0,\infty), H^2(\mathbb{T}^n))^N$ from Theorem 4, is a positive, global, weak solution to Equation (1.1).*

In particular, in one spatial dimension the solutions are classical and strictly positive, as proved in the following.

Theorem 6. *On* 1*D domains, the solution to Equation* (1.1) *given in Theorem 5 is a classical strictly positive solution.*

Proof. In one spatial dimension we have the Sobolev embedding from H^2 to C^1. By using the same argument of [17, Lemma 3.8], we can show that the solution u given in Theorem 5 is such that $u(\cdot, t) \in C^2$. Therefore, in 1D the solution to Equation (1.1) satisfies

$$u \in C^1((0,\infty), L^2(\mathbb{T}))^N \cap C^0([0,\infty), C^2(\mathbb{T}))^N, \tag{4.4}$$

which is therefore a classical solution. To prove that this solution is strictly positive in 1D, we consider the following linear parabolic PDE problem

$$\sigma_{it} = D_i \partial_{xx}\sigma_i + \partial_x\left(\sigma_i \sum_{j=1}^{N} \gamma_{ij}\partial_x(K_{ij} * u_j)\right), \qquad i = 1,\dots,N, \tag{4.5}$$

where $u = (u_1, \dots, u_N)$ is the solution to the one dimensional version of Equation (1.1) satisfying (4.4). Notice that the coefficients of the linear problem in Equation (4.5) are continuous. Let $\sigma = (\sigma_1, \dots, \sigma_N)$ be a non-negative (component-wise) classical solution to Equation (4.5). Then Harnack's inequality for parabolic systems (see [13, Theorem 10, page 370]) ensures that for each $0 < t_1 < t_2$ there exists a positive constant C such that

$$\sup_{\mathbb{T}} \sigma_i(x, t_1) \le C \inf_{\mathbb{T}} \sigma_i(x, t_2), \qquad i = 1,\dots,N. \tag{4.6}$$

In particular, $u = (u_1, \dots, u_N)$ is a solution to Equation (4.6), and therefore it satisfies the inequalities in Equation (4.6), that is

$$\sup_{\mathbb{T}} u_i(x, t_1) \le C \inf_{\mathbb{T}} u_i(x, t_2), \qquad i = 1,\dots,N, \tag{4.7}$$

for each $0 < t_1 < t_2$. Since $u_i \ge 0$ and $\|u_i\|_{L^1} = \|u_{i0}\|_{L^1} > 0$, it follows that $\sup u_i(x, t_1) > 0$, which implies that $\inf u_i(x, t) > 0$ at any positive time t. The above Harnack's inequality is not available for weak solutions in higher dimensions, hence we prove strict positivity only for the 1D case. □

5. Blow-up of the solutions in the local limit

In this section we formally show that solutions of the local version of Equation (1.1) (i.e., the equation obtained by choosing the kernels K_{ij} equal to the δ-Dirac function) can have finite time blow-up solutions for $n \ge 2$, where n denotes the spatial dimension. To this end, we use an argument previously used for chemotaxis models (see [33]). Namely, we consider a case where an aggregation arises at a certain location and we orient the torus $\mathbb{T}^n$ in such a way that the 'boundary' locations – i.e. where $x_k = \pm L_k/2$ for some k where $x = (x_1, \dots, x_n)$ – are far away from this aggregation. Then we consider the second moment of this aggregate and show that for a bounded solution, the second moment becomes negative over time. This contradicts the assumption of the solution to be bounded and hence implies blow-up. We will consider two cases: $\gamma_{ij} < 0$, for all $i, j = 1, \dots, N$ (mutual attraction and self-attraction); $\gamma_{ii} < 0$, $i = 1, \dots, N$ (self-attraction) and $\gamma_{ij} > 0$, $i \ne j$ (mutual avoidance).

Theorem 7 (Formal Blow-up)**.** *Consider the PDE*

$$u_{it} = D_i \Delta u_i + \nabla \cdot \left(u_i \sum_{j=1}^{N} \gamma_{ij} \nabla u_j \right), \tag{5.1}$$

obtained from Equation (1.1) *with* $K_{ij} = \delta$*, for all* $i, j = 1, \ldots, N$*, where* δ *denotes the* δ*-Dirac distribution. Let*

$$P := \sum_{i=1}^{N} \int_{\mathbb{T}^n} u_{i0}(x) dx, \quad \gamma^{(ij)} := \max_{i,j=1,\ldots,N} \{\gamma_{ij}\}, \quad \gamma^{(ii)} := \max_{i=1,\ldots,N} \{\gamma_{ii}\}, \quad D := \max_{i=1,\ldots,N} \{D_i\}. \tag{5.2}$$

Assume that $\boldsymbol{u}(x,t) = (u_1(x,t), u_2(x,t), \ldots, u_N(x,t))$ *is the solution with initial condition* $\boldsymbol{u}_0 = (u_{10}, \ldots, u_{N0})$*. Assume further that, for all* $i = 1, \ldots, N$*,* u_{i0} *decays to zero as* $x_k \to -L_k, L_k$ *for any* $k = 1, \ldots, n$*.*

Case 1. *Let* $\gamma_{ij} < 0$ *(mutual and self- attraction), for all* $i, j = 1, \ldots, N$*. If*

$$P > \frac{|\mathbb{T}^n|}{2} \quad \text{and} \quad \gamma^{(ij)} < -\frac{2PD}{2P - |\mathbb{T}^n|} \tag{5.3}$$

then the solution $\boldsymbol{u}$ *becomes unbounded in finite time.*

Case 2. *Let* $\gamma_{ii} < 0$ *(self-attraction), for* $i = 1, \ldots, N$*, and* $\gamma_{ij} > 0$ *(mutual avoidance), for* $i \neq j$ *and* $i, j = 1, \ldots, N$*, such that*

$$\sum_{\substack{j=1 \\ j \neq i}}^{N} (\gamma_{ij} + \gamma_{ji}) < -\gamma_{ii}, \quad \text{for all} \quad i = 1, \ldots, N. \tag{5.4}$$

If

$$P > N\frac{|\mathbb{T}^n|}{2} \quad \text{and} \quad \gamma^{(ii)} < -\frac{4PD}{2P - N|\mathbb{T}^n|}, \tag{5.5}$$

then the solution $\boldsymbol{u}$ *becomes unbounded in finite time.*

Proof. **Case 1.** Define the second moment as

$$M(t) := \sum_{i=1}^{N} \int_{\mathbb{T}^n} |x|^2 u_i(x,t) dx, \tag{5.6}$$

and compute

$$
\begin{aligned}
\frac{d}{dt}M &= \sum_{i=1}^{N}\int_{\mathbb{T}^n}|x|^2u_{it}dx \\
&= \sum_{i=1}^{N}D_i\int_{\mathbb{T}^n}|x|^2\Delta u_i dx + \sum_{i,j=1}^{N}\gamma_{ij}\int_{\mathbb{T}^n}|x|^2\nabla\cdot(u_i\nabla u_j)dx \\
&= \sum_{i=1}^{N}D_i\left(\int_{\mathbb{T}^n}\nabla\cdot(|x|^2\nabla u_i)dx - \int_{\mathbb{T}^n}\nabla(|x|^2)\cdot\nabla u_i dx\right)dx \\
&\quad + \sum_{i,j=1}^{N}\gamma_{ij}\left(\int_{\mathbb{T}^n}\nabla\cdot(|x|^2u_i\nabla u_j)_x dx - \int_{\mathbb{T}^n}\nabla(|x|^2)\cdot(u_i\nabla u_j)dx\right) \\
&= -\sum_{i=1}^{N}D_i\int_{\mathbb{T}^n}\nabla(|x|^2)\cdot\nabla u_i dx - \sum_{i,j=1}^{N}\gamma_{ij}\int_{\mathbb{T}^n}\nabla(|x|^2)\cdot(u_i\nabla u_j)dx \\
&= -2\sum_{i=1}^{N}D_i\int_{\mathbb{T}^n}x\cdot\nabla u_i dx - 2\sum_{i,j=1}^{N}\gamma_{ij}\int_{\mathbb{T}^n}x\cdot(u_i\nabla u_j)dx \\
&= -2\sum_{i=1}^{N}D_i\int_{\mathbb{T}^n}x\cdot\nabla u_i dx - \sum_{i,j=1}^{N}\gamma_{ij}\int_{\mathbb{T}^n}x\cdot\nabla(u_iu_j)dx \\
&= -2\sum_{i=1}^{N}D_i\int_{\mathbb{T}^n}\nabla\cdot(xu_i)dx + 2n\sum_{i=1}^{N}D_i\int_{\mathbb{T}^n}u_i\,dx - \sum_{i,j=1}^{N}\gamma_{ij}\int_{\mathbb{T}^n}\nabla\cdot(xu_iu_j)\,dx + n\sum_{i,j=1}^{N}\gamma_{ij}\int_{\mathbb{T}^n}u_iu_j\,dx \\
&= 2n\sum_{i=1}^{N}D_i\int_{\mathbb{T}^n}u_i\,dx + n\sum_{i,j=1}^{N}\gamma_{ij}\int_{\mathbb{T}^n}u_iu_j\,dx \\
&\le 2n\sum_{i=1}^{N}D_i\int_{\mathbb{T}^n}u_i\,dx + \gamma^{(ii)}n\sum_{i,j=1}^{N}\int_{\mathbb{T}^n}u_iu_j\,dx \\
&= 2n\sum_{i=1}^{N}D_i\int_{\mathbb{T}^n}u_i dx + \gamma^{(ii)}n\int_{\mathbb{T}^n}\left(\sum_{i=1}^{N}u_i\right)^2 dx \\
&\le 2Dn\sum_{i=1}^{N}\int_{\mathbb{T}^n}u_i dx + \gamma^{(ii)}n\int_{\mathbb{T}^n}\left(\sum_{i=1}^{N}u_i\right)^2 dx \\
&\le 2Dn\sum_{i=1}^{N}\int_{\mathbb{T}^n}u_i dx + \gamma^{(ii)}n\left(2\sum_{i=1}^{N}\int_{\mathbb{T}^n}u_i dx - |\mathbb{T}^n|\right) \\
&= 2Dn\sum_{i=1}^{N}\int_{\mathbb{T}^n}u_{i0} dx + \gamma^{(ii)}n\left(2\sum_{i=1}^{N}\int_{\mathbb{T}^n}u_{i0} dx - |\mathbb{T}^n|\right)
\end{aligned}
\tag{5.7}
$$

where $\gamma^{(ii)}$ and D are defined in Equation (5.2). The third and seventh equalities are obtained integrating by parts. The third inequality follows from $\gamma^{(ii)} < 0$ and the Young's inequality $a^2 \ge 2a - 1$. The last equality follows from conservation of total population size, i.e. $\int_{\mathbb{T}^n}u_i(x,t)dx = \int_{\mathbb{T}^n}u_{i0}(x)dx$, for all $t \ge$

0, where u_{i0} is the initial condition.

By using the definition of $P = \sum_{i=1}^{N} \int_{\mathbb{T}^n} u_{i0}(x)dx$, Equation (5.7) can be rewritten as

$$\frac{d}{dt}M \leq 2DnP + \gamma^{(ii)} n \left(2P - |\mathbb{T}^n|\right). \tag{5.8}$$

Since

$$P > \frac{|\mathbb{T}^n|}{2} \text{ and } \gamma^{(ii)} = -\frac{2PD + \varepsilon}{2P - |\mathbb{T}^n|}, \tag{5.9}$$

for some $\varepsilon > 0$, then $\frac{d}{dt}M < -\varepsilon n$. Since the derivative of $M(t)$ is bounded above by a strictly negative constant, $-\varepsilon n$, there exists a finite time $T > 0$ such that $M(T) = 0$ (by Mean Value Theorem). Hence, by Equation (5.6) and since $u_i(x,t)$ conserves its total mass, it follows that, for all $i = 1, \ldots, N$, u_i tends to $\delta(x)$, the Dirac delta function, as $t \to T$. This completes the proof of **Case 1.**

Case 2. As in the previous case, we compute the time-derivative of the second moment of $M(t)$ as follows

$$\begin{aligned}
\frac{d}{dt}M &= 2n \sum_{i=1}^{N} D_i \int_{\mathbb{T}^n} u_i \, dx + n \sum_{i,j=1}^{N} \gamma_{ij} \int_{\mathbb{T}^n} u_i u_j \, dx \\
&= 2n \sum_{i=1}^{N} D_i \int_{\mathbb{T}^n} u_i \, dx + n \sum_{i=1}^{N} \gamma_{ii} \int_{\mathbb{T}^n} u_i^2 \, dx + n \sum_{\substack{i,j=1 \\ i \neq j}}^{N} \gamma_{ij} \int_{\mathbb{T}^n} u_i u_j \, dx \\
&\leq 2n \sum_{i=1}^{N} D_i \int_{\mathbb{T}^n} u_i \, dx + n \sum_{i=1}^{N} \gamma_{ii} \int_{\mathbb{T}^n} u_i^2 \, dx + \frac{n}{2} \sum_{\substack{i,j=1 \\ i \neq j}}^{N} (\gamma_{ij} + \gamma_{ji}) \int_{\mathbb{T}^n} u_i^2 \, dx \\
&\leq 2n \sum_{i=1}^{N} D_i \int_{\mathbb{T}^n} u_i \, dx + \frac{n}{2} \sum_{i=1}^{N} \gamma_{ii} \int_{\mathbb{T}^n} u_i^2 \, dx \\
&\leq 2Dn \sum_{i=1}^{N} \int_{\mathbb{T}^n} u_i \, dx + \gamma^{(ii)} \frac{n}{2} \sum_{i=1}^{N} \int_{\mathbb{T}^n} u_i^2 \, dx \\
&\leq 2Dn \sum_{i=1}^{N} \int_{\mathbb{T}^n} u_i dx + \gamma^{(ii)} \frac{n}{2} \sum_{i=1}^{N} \int_{\mathbb{T}^n} (2u_i - 1) dx \\
&= 2Dn \sum_{i=1}^{N} \int_{\mathbb{T}^n} u_i dx + \gamma^{(ii)} n \sum_{i=1}^{N} \int_{\mathbb{T}^n} u_i dx - \gamma^{(ii)} \frac{n}{2} N |\mathbb{T}^n| \\
&= 2Dn \sum_{i=1}^{N} \int_{\mathbb{T}^n} u_{i0} dx + \gamma^{(ii)} n \sum_{i=1}^{N} \int_{\mathbb{T}^n} u_{i0} dx - \gamma^{(ii)} \frac{n}{2} N |\mathbb{T}^n|,
\end{aligned} \tag{5.10}$$

where $\gamma^{(ii)}$ and D are defined in Equation (5.2). Since $P = \sum_{i=1}^{N} \int_{\mathbb{T}^n} u_{i0}(x)dx$, Equation (5.10) can be rewritten as

$$\frac{d}{dt}M \leq 2DnP + \gamma^{(ii)} n \left(P - \frac{N}{2}|\mathbb{T}^n|\right). \tag{5.11}$$

Since

$$P > N\frac{|\mathbb{T}^n|}{2} \text{ and } \gamma^{(ii)} = -\frac{4PD + \varepsilon}{2P - N|\mathbb{T}^n|}, \tag{5.12}$$

for some $\varepsilon > 0$, then $\frac{d}{dt}M < -\varepsilon n/2$. Then, by the same argument as **Case 1**, u_i tends to $\delta(x)$ as $t \to T$, for all $i = 1, \ldots, N$. □

The above calculations do not give a complete categorisation of blow-up regimes, but do demonstrate the singular nature of non-linear and local cross-diffusion terms. As with chemotaxis models [1, 22, 23, 25], such a categorisation requires advanced machinery such as energy estimates or multiscale arguments, which are beyond the scope of this work. We leave the general question of blow-up in Equation (5.1) as an interesting open problem.

6. Numerical simulations

The aim of this section is to demonstrate numerically how the existence of solutions breaks down in the spatially-local limit of Equation (1.1) for a few choice examples. For our numerical solutions, we use a spectral method and the numerical scheme described in [17]. First, we analyse the behaviour of the numerical solutions when adopting the following interaction kernel:

$$K_{ij}(x, y) = \begin{cases} \frac{\pi}{r_{ij}^2(\pi^2-4)}\left(1 + \cos\left(\frac{\pi}{r_{ij}}\sqrt{x^2+y^2}\right)\right), & \text{if } x^2 + y^2 \le r_{ij}^2, \\ 0, & \text{otherwise,} \end{cases} \tag{6.1}$$

which satisfies the assumptions of Theorem 2.

Figure 1 shows three sets of numerical simulations obtained by fixing $N = 1$ population (in (a) and (b)), $N = 2$ populations (in (c) and (d)) and $N = 3$ populations (in (e) and (f)), with $\gamma_{ij} < 0$ (mutual attraction) and $r_{ij} = r_{ji}$, for all i, j. The simulated populations become steeper as the detection radius, r_{ij}, decreases. This is suggestive of blow-up as r_{ij} vanishes, even though solutions remain bounded for all strictly positive r_{ij}. Note that in the limit $r_{ij} \to 0$ for all i and j, this example reduces to **Case 1** analysed in the previous section. There, we show that the local system may undergo a finite time blow-up for large enough initial data. The appearance of spike solutions becomes more pronounced with the addition of populations. In fact, for fixed values of r_{ij}, the addition of populations makes the solution higher and steeper, due to the fact that, in addition to self-attraction, the populations also exhibit mutual attraction (compare panels a, c, and e).

Figure 2 shows a similar analysis to Figure 1, but this time focusing on the situation relevant to **Case 2**, i.e. populations exhibiting mutual avoidance and a sufficiently strong self-attraction. As with Figure 1, we observe that as r_{ij} decreases, the population profiles become steeper, suggesting blow-up as r_{ij} tends to zero.

Case 1. $\gamma_{ij} < 0$: Self attraction and Mutual attraction

N = 1

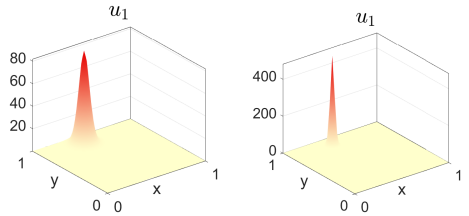

(a) $r_{11} = 0.3$ **(b)** $r_{11} = 0.2$

N = 2

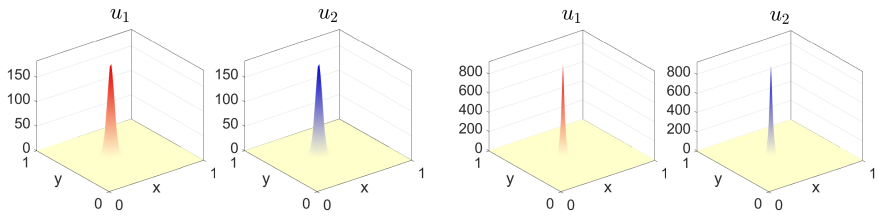

(c) $r_{ij} = 0.3$ **(d)** $r_{ij} = 0.2$

N = 3

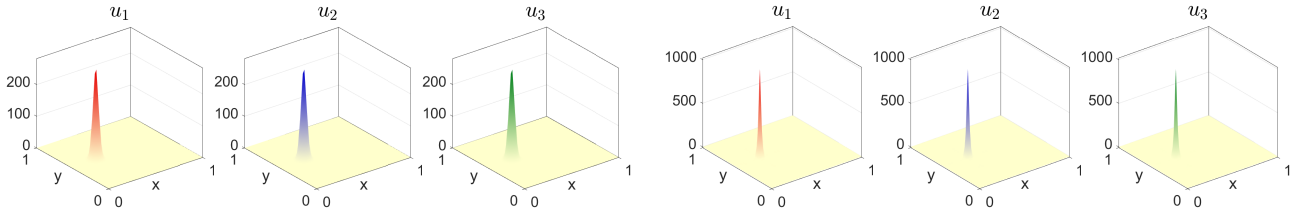

(e) $r_{ij} = 0.3$ **(f)** $r_{ij} = 0.2$

Figure 1. Numerical simulations of Equations (1.1), with K_{ij} defined as in (6.1), on square domains for different numbers N of populations: $N = 1$ in (a)-(b), $N = 2$ in (c)-(d), and $N = 3$ in (e)-(f), for decreasing values of the sensing ranges r_{ij}, with $r_{ij} = r_{ji}$, for $i, j = 1, 2, 3$. The other parameter values are: $D_i = 1$, $\gamma_{ij} = \gamma_{ji} = -1$, for all $i, j = 1, 2, 3$. For each value of N, the stationary states with $r_{ij} = 0.3$ (panels (a), (c), and (e)) emerge from a small random perturbation of the homogeneous steady state. The resulting stationary solution is then used as the initial condition for the simulation with $r_{ij} = 0.2$. All panels show the solutions at time $T = 10$, after transient dynamics have subsided.

Case 2. $\gamma_{ii} < 0$, $\gamma_{ij} > 0$ for $i \neq j$: Self attraction and Mutual avoidance

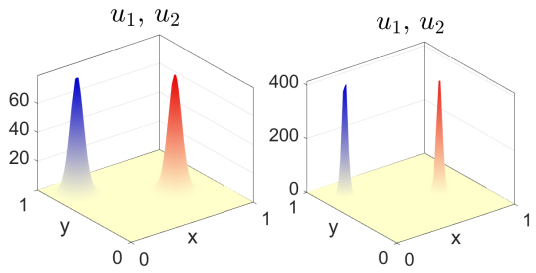

(a) $r_{ij} = 0.3$ **(b)** $r_{ij} = 0.2$

Figure 2. Numerical simulations of Equations (1.1), with K_{ij} defined as in (6.1), on square domains with $N = 2$, for decreasing values of the sensing ranges r_{ij}, with $r_{ij} = r_{ji}$, for $i, j = 1, 2$. The other parameter values are: $D_1 = D_2 = 1$, $\gamma_{11} = \gamma_{22} = -5$, $\gamma_{12} = \gamma_{21} = 1$. The stationary solution in (a) emerges from a small random perturbation of the homogeneous steady state with $r_{ij} = 0.3$. This stationary solution is then used as the initial condition for the simulation with $r_{ij} = 0.2$ (panel (b)). All panels show the solutions at time $T = 10$, after transient dynamics have subsided.

In addition to these two examples inspired by the **Case 1** and **Case 2**, we also examine some cases where we do not currently have blow-up results. For example, Figure 3 shows the case of two populations that attract each other ($\gamma_{12}, \gamma_{21} < 0$) but do not exhibit self-attraction ($\gamma_{ii} = 0$). Likewise, in Figure 4 we consider a mixture of self-avoidance and self-attraction, mutual avoidance and mutual attraction, again observing a peak narrowing as r_{ij} decreases. Note also that, in Figures 3 and 4, only one of the detection radii is reduced, suggesting that solutions of System (1.1) may blow-up even in situations where just one of the kernels K_{ij} is the δ-Dirac function. A detailed analysis of various blow-up scenarios is a fruitful direction of future research.

Case 3. $\gamma_{ii} = 0$, $\gamma_{ij} < 0$ for $i \neq j$: No-Self attraction and Mutual attraction

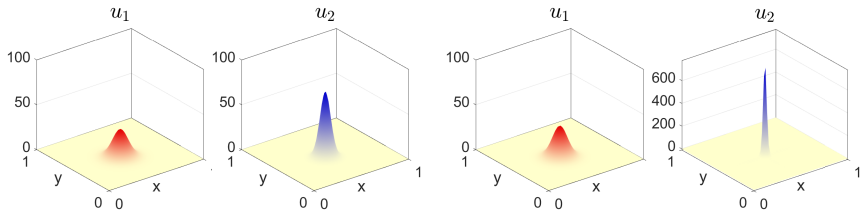

(a) $r_{2j} = 0.3$ **(b)** $r_{2j} = 0.1$

Figure 3. Numerical simulations of Equations (1.1), with K_{ij} defined as in (6.1), on square domains with $N = 2$, for decreasing values of the sensing ranges $r_{21} = r_{22}$, with $r_{11} = r_{12} = 0.4$ fixed. The other parameter values are: $D_1 = D_2 = 1$, $\gamma_{11} = \gamma_{22} = 0$, $\gamma_{12} = \gamma_{21} = -1.2$, $\gamma_{12} = \gamma_{21} = 1$. The stationary solution in (a) emerges from a small random perturbation of the homogeneous steady state with $r_{ij} = 0.3$. This resulting stationary solution is then used as the initial condition for the simulation with $r_{ij} = 0.1$ (panel (b)). All panels show the solutions at time $T = 10$, after transient dynamics have subsided.

Case 4. Miscellaneous

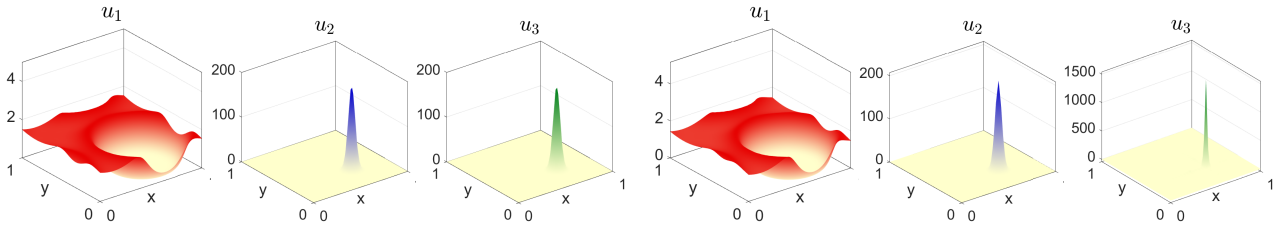

(a) $r_{3j} = 0.3$ **(b)** $r_{3j} = 0.1$

Figure 4. Numerical simulations of Equations (1.1), with K_{ij} defined as in (6.1), on square domains with $N = 3$ for decreasing values of the sensing ranges $r_{31} = r_{32} = r_{33}$, while $r_{1j} = 0.4$ and $r_{2j} = 0.3$, for $j = 1, 2, 3$, are kept fixed. The other parameter values are: $D_1 = D_2 = D_3 = 1$, $\gamma_{11} = 1$, $\gamma_{22} = -1$, $\gamma_{33} = -1$, $\gamma_{12} = \gamma_{21} = 1$, $\gamma_{13} = \gamma_{31} = 1$, $\gamma_{23} = \gamma_{32} - 1$. The stationary solution in (a) emerges from a small random perturbation of the homogeneous steady state with $r_{ij} = 0.3$. This resulting stationary solution is then used as the initial condition for the simulation with $r_{ij} = 0.1$ (panel (b)). All panels show the solutions at time $T = 30$, after transient dynamics have subsided.

To assess the consistency of the observed steepening behaviour with respect to the choice of kernel, we performed additional simulations using two alternative smooth kernels: the following bump kernel

$$K(x,y) = \begin{cases} C\left(e^{-\frac{|\mathbf{x}|^2/r^2}{\sigma^2(1-|\mathbf{x}|^2/r^2)}}\right), & \text{if } |\mathbf{x}|^2 = x^2 + y^2 \le r^2, \\ 0, & \text{otherwise,} \end{cases} \tag{6.2}$$

and the following mollified top-hat kernel

$$K(x,y) = \begin{cases} C_1, & \text{if } x^2 + y^2 < r_I^2, \\ C_1 \exp\left(1 - \frac{1}{1-\left(\frac{|\mathbf{x}|-r_I}{r-r_1}\right)^2}\right), & \text{if } r_I^2 \le x^2 + y^2 < r^2, \\ 0, & \text{otherwise.} \end{cases} \tag{6.3}$$

Both kernels are supported on a disk of radius r and satisfy the assumptions of Theorem 2. The constants C and C_1 in the kernel definitions are chosen so that the resulting functions are probability densities, i.e., they integrate to one over their support, and we set $\sigma = 0.5$ and $r_I = 0.9r$ throughout. We carried out a similar investigation to that of the cosine kernel (Equation (6.1)) and observed comparable steepening behaviour for decreasing values of the interaction range r. Here, we present results for a representative case: the two-population setting under Case 1, where $\gamma_{ij} < 0$, and $r_{ij} = r_{ij} =: r$, for all i, j. In our simulations, we observe that, as r decreases, the stationary solutions become increasingly peaked (see Figure 5), suggesting a tendency towards blow-up in the local limit. However, the rate at which this steepening occurs depends on the kernel. Specifically, the bump kernel produces sharper peaks more quickly as r decreases (see Figure 5 (a) and (b)), whereas the smooth top-hat kernel produces a more gradual increase in peak height (see Figure 5(c)-(e)). This difference appears to be related to the shape of the kernel, with more sharply concentrated kernels inducing stronger local

aggregation effects (see Figure 6). Overall, the simulations confirm that the steepening phenomenon is not specific to the cosine kernel and persists across a range of smooth, compactly supported interaction kernels.

Increasing the values of the diffusion coefficients tends to inhibit peak formation, eventually driving the system towards a homogeneous distribution. For this reason, in our simulations, we selected the diffusion coefficients D_i sufficiently small and the interaction strengths $|\gamma_{ij}|$ sufficiently large to ensure that the homogeneous steady state is linearly unstable, as shown in [19]. A small diffusion coefficient is necessary not only for this linear instability but also for the blow-up phenomenon described in Theorem 7, although the two regions are distinct. Indeed, there are cases where the homogeneous steady state is stable, yet stable steady state solutions also exist with steep peaks [18].

Case 1. $\gamma_{ij} < 0$: Self attraction and Mutual attraction for different kernels

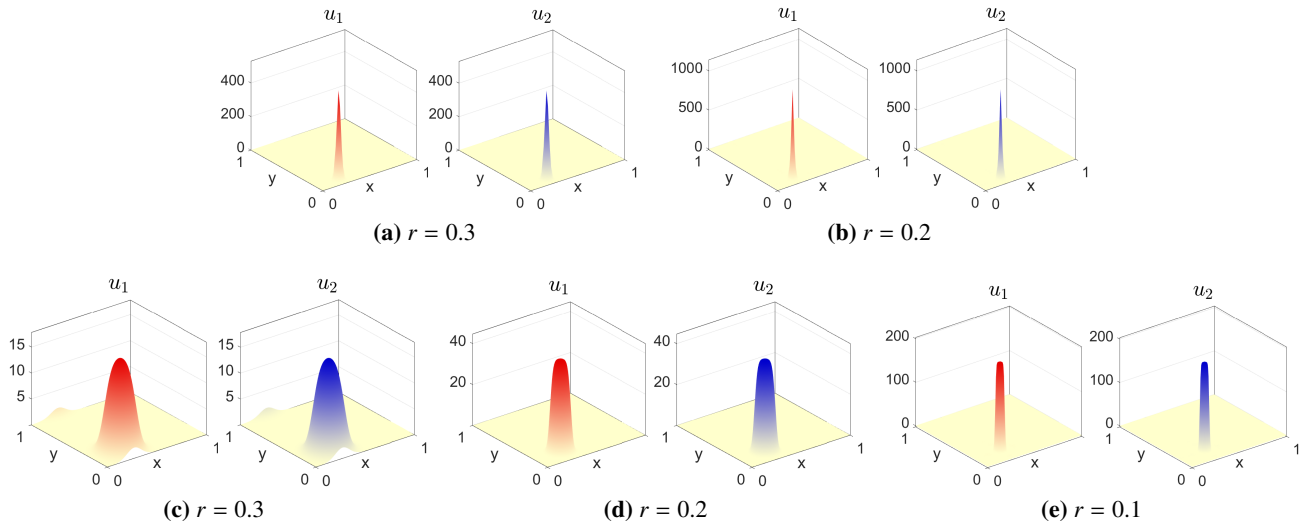

(a) $r = 0.3$ **(b)** $r = 0.2$ **(c)** $r = 0.3$ **(d)** $r = 0.2$ **(e)** $r = 0.1$

Figure 5. Numerical solutions of Equations (1.1), with $N = 2$ and $r := r_{ij} = r_{ji}$, for $i, j = 1, 2$. In (a)-(b): K is defined as in (6.2) with $\sigma = 0.5$; in (c)-(e): K is defined as in (6.3) with $r_I = 0.9r$. The other parameter values are: $D_i = 1$, $\gamma_{ij} = \gamma_{ji} = -1$, for all $i, j = 1, 2$. In each set of simulations, the stationary solution shown for $r = 0.3$ emerges from a small random perturbation of the homogeneous steady state. This stationary state is then used as initial condition for the simulations with $r = 0.2$ and $r = 0.1$. All panels show the solutions at time $T = 10$, after transient dynamics have subsided.

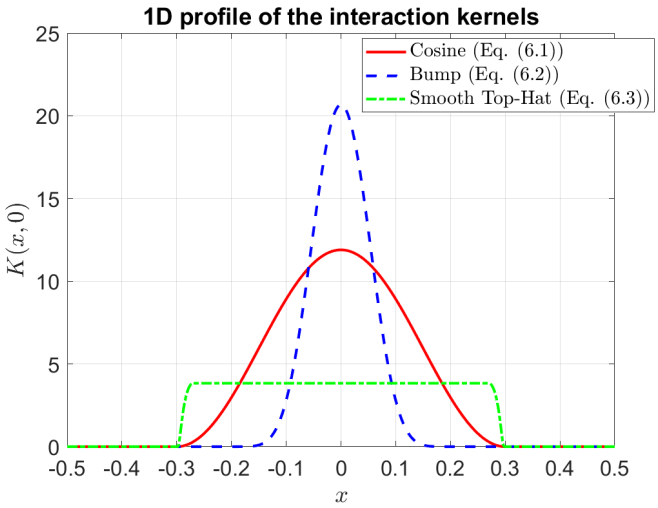

Figure 6. One-dimensional profiles of the three interaction kernels used in the simulations: cosine kernel in red (Equations (6.1)), bump kernel in blue (Equation (6.2)) and smooth top-hat kernel in green (Equation (6.3)), all supported on a disk of radius $r = 0.3$. For the bump kernel, we used $\sigma = 0.5$; for the smooth top-hat kernel, $r_I = 0.9r$. Each kernel is normalized so that its integral over the disk equals one.

7. Conclusions

We have established a comprehensive framework for understanding nonlocal advection-diffusion models of any number of interacting populations, which unifies and extends many previous results on existence of solutions, together with insights into blow-up of singular situations. We have shown that, under the assumption of sufficiently smooth kernels, positive solutions exist globally in any spatial dimension. This finding not only generalises existing knowledge, but also reveals a remarkable contrast with local models, where global existence often depends critically on the dimension of the spatial domain [10, 30, 38].

We also provide strong evidence for the critical role of nonlocal interactions in preventing the blow-up of solutions in finite time. Our analysis in Section 5 highlights the role of local cross-diffusion terms and their ability to create sudden singularities in finite time. Similar phenomena have been observed and analysed in chemotaxis models [1, 22, 26]. While a complete categorisation of blow-up would require sophisticated tools beyond the scope of this paper, the analysis of local limits and numerical simulations provide solid support for the crucial role of nonlocality in preventing blow-up, paving the way for future explorations of the long-term behaviour and applications of these models in a variety of fields.

From a practical perspective, existence and blow-up results can be very useful in informing users of PDE models whether they are sensibly defined. In particular, when performing numerics, knowledge of existence and blow-up regimes can inform whether those numerics are likely to produce meaningful results *a priori*, regardless of the numerical scheme being used. Here, we demonstrate how our insights on existence and blow-up translate to the appearance of spike-like solutions as the detection radius decreases to zero. As the limit is approached, it is necessary to use ever-higher spatial resolution to

capture the behaviour of the PDE accurately. However, away from this limit, solutions are nicely mollified, allowing for more rapid numerical analysis.

The general global existence result presented here paves the way to a systematic analysis of nonlocal biological interactions. Our main interest is to gain a better understanding of animal space use and oriented animal movement. Possible applications of the model (1.1) are widespread, including animal home ranges [2], space use by territorial competitors [36], swarming and flocking [11], species reactions to anthropogenic disturbances [31], and biodiversity in heterogeneous environments [39]. The results presented here put us at ease to freely use nonlocal PDE models of type (1.1) to describe complex spatio-temporal interactions arising from such applications.

Author contributions

Valeria Giunta: formal analysis, investigation, writing-original draft, writing-reviewing & editing; Thomas Hillen: conceptualization, formal analysis, methodology, writing-original draft, writing-reviewing & editing; Mark A. Lewis: conceptualization, writing-reviewing & editing; Jonathan R. Potts: conceptualization, formal analysis, writing-original draft, writing-reviewing & editing.

Use of Generative-AI tools declaration

The authors declare they have not used Artificial Intelligence (AI) tools in the creation of this article.

Acknowledgments

We thank various anonymous reviewers who provided comments on a previous version of our manuscript. JRP and VG acknowledge support of Engineering and Physical Sciences Research Council (EPSRC) grant EP/V002988/1 awarded to JRP. VG is also grateful for support from the National Group of Mathematical Physics (GNFM-INdAM). TH is supported through a discovery grant of the Natural Science and Engineering Research Council of Canada (NSERC), RGPIN-2023-04269. MAL gratefully acknowledges support from NSERC Discovery Grant RGPIN-2018-05210 and from the Gilbert and Betty Kennedy Chair in Mathematical Biology.

Conflict of Interest

The authors declare they have no competing interests in this paper.

References

1. N. Bellomo, A. Bellouquid, Y. Tao, M. Winkler, Toward a mathematical theory of Keller–Segel models of pattern formation in biological tissues, *Math. Mod. Meth. Appl. Sci.*, **25** (2015), 1663–1763. https://doi.org/10.1142/S021820251550044X
2. B. K. Briscoe, M. A. Lewis, S. E. Parrish, Home range formation in wolves due to scent marking, *B. Math. Biol.*, **64** (2002), 261–284. https://doi.org/10.1006/bulm.2001.0273

3. M. Burger, M. D. Francesco, S. Fagioli, A. Stevens, Sorting phenomena in a mathematical model for two mutually attracting/repelling species, *SIAM J. Math. Anal.*, **50** (2018), 3210–3250. https://doi.org/10.1137/17M1125716
4. A. Buttenschön, T. Hillen, *Non-Local Cell Adhesion Models*, Springer, 2021. https://doi.org/10.1007/978-3-030-67111-2
5. J. Carrillo, Y. Choi, M. Hauray. The derivation of swarming models: Mean filed limit and Wasserstein distances, In *Collective Dynamics from Bacteria to Crowds*, (2014), 1–46. Springer. https://doi.org/10.1007/978-3-7091-1785-9_1
6. J. Carrillo, R. Galvani, G. Pavliotis, A. Schlichting, Long-time behavior and phase transitions for the McKean-Vlasov equation on a torus, *Archives Rational Mechanics and Analysis*, **235** (2020), 635–690. https://doi.org/10.1007/s00205-019-01430-4
7. J. A. Carrillo, A. Colombi, M. Scianna, Adhesion and volume constraints via nonlocal interactions determine cell organisation and migration profiles, *J. Theor. Biol.*, **445** (2018), 75–91. https://doi.org/10.1016/j.jtbi.2018.02.022
8. J. A. Carrillo, R. S. Gvalani, Phase transitions for nonlinear nonlocal aggregation-diffusion equations, *Commun. Math. Phys.*, **382** (2021), 485–545. https://doi.org/10.1007/s00220-021-03977-4
9. B. Chazelle, Q. Jiu, Q. Li, C. Wang, Well-posedness of the limiting equation of a noisy consensus model in opinion dynamics, *J. Differ. Equations*, **263** (2017), 365–397. https://doi.org/10.1016/j.jde.2017.02.036
10. D. Gilbarg, N. Trudinger *Elliptic Partial Differential Equations of Second Order*, Springer, Heidelberg, 1977. https://doi.org/10.1007/978-3-642-96379-7
11. R. Eftimie, *Hyperbolic and kinetic models for self-organised biological aggregations*, Springer, 2018. https://doi.org/10.1007/978-3-030-02586-1
12. R. Eftimie, G. de Vries, M. A. Lewis, Complex spatial group patterns result from different animal communication mechanisms, *Proceedings of the National Academy of Sciences*, **104** (2007), 6974–6979. https://doi.org/10.1073/pnas.0611483104
13. L. C. Evans, *Partial differential equations*, volume 19, American Mathematical Society, 2022.
14. W. F. Fagan, E. Gurarie, S. Bewick, A. Howard, R. S. Cantrell, C. Cosner, Perceptual ranges, information gathering, and foraging success in dynamic landscapes, *The American Naturalist*, **189** (2017), 474–489. https://doi.org/10.1086/691099
15. R. C. Fetecau, Y. Huang, T. Kolokolnikov, Swarm dynamics and equilibria for a nonlocal aggregation model, *Nonlinearity*, **24** (2011), 2681. https://doi.org/10.1088/0951-7715/24/10/002
16. S. Genieys, V. Volpert, P. Auger, Pattern and waves for a model in population dynamics with nonlocal consumption of resources, *Math. Model. Nat. Pheno.*, **1** (2006), 63–80. https://doi.org/10.1051/mmnp:2006004
17. V. Giunta, T. Hillen, M. Lewis, J. R. Potts, Local and global existence for nonlocal multispecies advection-diffusion models, *SIAM J. Appl. Dyn. Syst.*, **21** (2022), 1686–1708. https://doi.org/10.1137/21M1425992

18. V. Giunta, T. Hillen, M. A. Lewis, J. R. Potts, Detecting minimum energy states and multi-stability in nonlocal advection–diffusion models for interacting species, *J. Math. Biol.*, **85** (2022), 1–44. https://doi.org/10.1007/s00285-022-01824-1

19. V. Giunta, T. Hillen, M. A. Lewis, J. R. Potts, Weakly nonlinear analysis of a two-species non-local advection-diffusion system, *Nonlinear Analysis: Real World Applications*, **78** (2024), 104086. https://doi.org/10.1016/j.nonrwa.2024.104086

20. T. Glimm, J. Zhang, Numerical approach to a nonlocal advection-reaction-diffusion model of cartilage pattern formation, *Math. Comput. Appl.*, **25** (2020), 36. https://doi.org/10.3390/mca25020036

21. T. Hillen, K. Painter, Global existence for a parabolic chemotaxis model with prevention of overcrowding, *Adv. Appl. Math.*, **26** (2001), 280–301. https://doi.org/10.1006/aama.2001.0721

22. T. Hillen, K. Painter, A user's guide to PDE models for chemotaxis, *J. Math. Biol.*, **58** (2009), 183–217. https://doi.org/10.1007/s00285-008-0201-3

23. T. Hillen, K. Painter, C. Schmeiser, Global existence for chemotaxis with finite sampling radius, *Discr. Cont. Dyn. Syst. B (DCDS-B)*, **7** (2007), 125–144. https://doi.org/10.3934/dcdsb.2007.7.125

24. T. Hillen, K. J. Painter, M. Winkler, Global solvability and explicit bounds for non-local adhesion models, *Eur. J. Appl. Math.*, **29** (2018), 645–684. https://doi.org/10.1017/S0956792517000328

25. D. Horstmann, From 1970 until present: The Keller-Segel model in chemotaxis and its consequences I, *Jahresberichte der DMV*, **105** (2003), 103–165.

26. D. Horstmann, K. J. Painter, H. G. Othmer, Aggregation under local reinforcement: From lattice to continuum, *Eur. J. Appl. Math.*, **15** (2004), 545–576. https://doi.org/10.1017/S0956792504005571

27. T. J. Jewell, A. L. Krause, P. K. Maini, E. A. Gaffney, Patterning of nonlocal transport models in biology: the impact of spatial dimension, *Math. Biosci.*, **366** (2023), 109093. https://doi.org/10.1016/j.mbs.2023.109093

28. A. Jüngel, S. Portisch, A. Zurek, Nonlocal cross-diffusion systems for multi-species populations and networks, *Nonlinear Analysis*, **219** (2022), 112800. https://doi.org/10.1016/j.na.2022.112800

29. M. A. Lewis, S. V. Petrovskii, J. R. Potts, *The mathematics behind biological invasions*, volume 44, Springer, 2016. https://doi.org/10.1007/978-3-319-32043-4

30. G. Lieberman, *Second Order Parabolic Differential Equations*, World Scientific, London, 1996. https://doi.org/10.1142/3302

31. K. Mokross, J. R. Potts, C. L. Rutt, P. C. Stouffer, What can mixed-species flock movement tell us about the value of amazonian secondary forests? Insights from spatial behavior, *Biotropica*, **50** (2018), 664–673. https://doi.org/10.1111/btp.12557

32. K. Painter, J. Potts, T. Hillen, Biological modelling with nonlocal advection diffusion equations, *Math. Mod. Meth. Appl. Sci. (M3AS)*, **34** (2024), 57–107. https://doi.org/10.1142/S0218202524400025

33. B. Perthame, *Transport Equations in Biology*, Birkhäuser, 2007. https://doi.org/10.1007/978-3-7643-7842-4

34. J. R. Potts, V. Giunta, M. A. Lewis, Beyond resource selection: emergent spatio–temporal distributions from animal movements and stigmergent interactions, *Oikos*, (2022), e09188. https://doi.org/10.1101/2022.02.28.482253

35. J. R. Potts, M. A. Lewis, How memory of direct animal interactions can lead to territorial pattern formation, *J. R. Soc. Interface*, **13** (2016), 20160059. https://doi.org/10.1098/rsif.2016.0059

36. J. R. Potts, M. A. Lewis, Territorial pattern formation in the absence of an attractive potential, *J. Math. Biol.*, **72** (2016), 25–46. https://doi.org/10.1007/s00285-015-0881-4

37. J. R. Potts, M. A. Lewis, Spatial memory and taxis-driven pattern formation in model ecosystems, *B. Math. Biol.*, **81** (2019), 2725–2747. https://doi.org/10.1007/s11538-019-00626-9

38. T. Suzuki, *Free Energy and Self-Interacting Particles*, Birkhaeuser, Basel, 2008.

39. D. Tilman, F. Isbell, J. M. Cowles, Biodiversity and ecosystem functioning, *Annu. Rev. Ecol. Evol. Syst.*, **45** (2014), 471–493. https://doi.org/10.1146/annurev-ecolsys-120213-091917

40. H. Wang, Y. Salmaniw, Open problems in pde models for knowledge-based animal movement via nonlocal perception and cognitive mapping, *J. Math. Biol.*, **86** (2023), 71. https://doi.org/10.1007/s00285-023-01905-9

AIMS Press